

# Influences of the Geopolymer Composition on the Strength and Durability of Fly Ash-based Geopolymer Stabilized Compacted Soil

Thanh-Phong Ngo<sup>1</sup>, Quoc-Bao Bui<sup>2</sup>, Vu To-Anh Phan<sup>3\*</sup>

<sup>1</sup> Faculty of Architecture-Construction, Thu Dau Mot University, Ho Chi Minh City 70000, Vietnam

<sup>2</sup> Sustainable Developments in Civil Engineering Research Group, Faculty of Civil Engineering, Ton Duc Thang University, Ho Chi Minh City 70000, Vietnam

<sup>3</sup> Smart Computing in Civil Engineering Research Group, Faculty of Civil Engineering, Ton Duc Thang University, Ho Chi Minh City 70000, Vietnam

\* Corresponding author, e-mail: [phantoanhvu@tdtu.edu.vn](mailto:phantoanhvu@tdtu.edu.vn)

Received: 28 September 2025, Accepted: 18 March 2026, Published online: 30 March 2026

## Abstract

Compacted earth materials are sustainable construction alternatives, but their durability is commonly enhanced using Portland cement, which has a high environmental impact. Geopolymers offer a potential low-carbon replacement and demonstrate promising mechanical properties, durability, and environmental performance. This study investigates the influence of geopolymer composition on the mechanical properties and durability of geopolymer-stabilized compacted earth (GSCE). Samples were prepared using  $\text{Na}_2\text{SiO}_3/\text{NaOH}$  ratios ranging from 1.0 to 2.0 with 10 M NaOH. In the first stage, compressive strength was optimized by varying curing temperature and curing time. The highest strength was obtained for specimens with a  $\text{Na}_2\text{SiO}_3/\text{NaOH}$  ratio of 1.5, cured at 90 °C for 24 h. In the second stage, durability was evaluated for GSCE prepared under these optimal conditions through wetting–drying cycles ( $C = 1\text{--}12$ ) in tap water, salt water, and acidic solution ( $\text{pH} = 4$ ). Under acidic conditions, compressive strength increased and reached a maximum after six wetting–drying cycles. XRD and FTIR analyses were used to identify phase development and chemical bonding within the geopolymer matrix. The results highlight the potential of geopolymer-stabilized compacted earth as a durable, environmentally sustainable construction material that incorporates industrial by-products.

## Keywords

geopolymer stabilized compacted earth, mechanical characteristics, wetting-drying cycles, compressive strength, molecular bond

## 1 Introduction

Portland cement is a popular binder of construction materials. However, the production of clinker (the main component of Portland cement) needs burning temperatures of about 1500 °C, which consumes high energy and releases consequent  $\text{CO}_2$  into the air [1]. In soil stabilization, Ordinary Portland cement has proved the improvement in geotechnical properties of stabilized soil as investigated by Asadoullahtabar et al. [2]. To reduce carbon emissions and energy consumption, scientific research and technological experts have been searching for alternative binders to replace cement in civil engineering materials.

Geopolymers have gained significant attention as a promising alternative to cement in recent years due to their potential to reduce carbon emissions and energy consumption. The geopolymer is obtained through chemical

reactions between aluminosilicate materials and alkaline solutions, which form a three-dimensional network structure [3]. Therefore, geopolymer can be a binder to replace Portland cement. The main advantage of geopolymer is its lower carbon footprint compared to Portland cement [4]. Moreover, the aluminosilicate sources for geopolymer can be taken from the industrial by-products (fly ash, slag, ...), which reduces environmental impacts. Geopolymer-based materials have interesting engineering properties, including high early strength, high durability, and good performance at high temperatures [5]. Therefore, applying geopolymer for earth materials exposed to severe climatic conditions (for example, in Southeast Asia) is an option that should be explored. The formulation of which has been well established, the compositions of geopolymer and

geopolymer-based materials have yet to be unified. Several studies have investigated the feasibility of geopolymer stabilization for earth materials [6]. Most of these studies investigate the influences of geopolymer composition (the substances in the creation of geopolymer) on the mechanical properties of earth materials. To our knowledge, the influences of the different compositions of geopolymer on the durability of geopolymer-stabilized earth materials have yet to be examined in detail. Indeed, among several factors that can influence the durability of geopolymer-stabilized earth, the  $\text{Na}_2\text{SiO}_3/\text{NaOH}$  (SS/SH) ratio is an important factor; this ratio is usually proposed in the range from 1 to 3 [7]. The curing temperature is also an important factor.

In practice, the application of geopolymers in stabilized soils faces several limitations, particularly the high energy demand associated with elevated-temperature curing and challenges related to scalability for field applications. These issues remain significant challenges for researchers. In addition, in southern Vietnam, saltwater intrusion has severely affected social life and local livelihoods. However, existing studies on civil engineering materials have primarily focused on mechanical performance and durability, with limited attention to the combined effects of saline and acidic environments and repeated wetting–drying cycles. Consequently, significant research gaps remain, underscoring the need for more comprehensive investigations. This study investigates the UCS of the geopolymer-stabilized compacted earth (GSCE) in two steps. First, the influences of curing time, curing temperature, and  $\text{Na}_2\text{SiO}_3/\text{NaOH}$  ratio on the compressive strength of GSCE have been examined. Then, the influences of these parameters on the compressive strength of GSCE after several wetting–drying (w-d) cycles in various solutions (tap water, salt water, and acid solution) were investigated. The XRD and FTIR techniques were employed to interpret the results. This study aims to contribute to understanding the effects of the  $\text{Na}_2\text{SiO}_3/\text{NaOH}$  ratio and curing temperature on the durability of GSCE exposed to w-d cycles.

## 2 Materials and methods

### 2.1 Materials used

#### 2.1.1 Soil characterization

This study used soil collected from a quarry in Binh Duong province, Vietnam. The basic properties of the soil were characterized following ASTM D6913/D6913M-17 [8]: the grain size distribution, specific gravity, Atterberg limits, and Proctor optimum water content. The results are

summarized in Table 1 [8–11]. Based on the Atterberg limits and the plasticity index, following the AASHTO M 145-91 (2012) [12], the soil is classified as low-plasticity clay. In a prior study [13], the soil sample's composition was detailed, revealing the presence of kaolinite, quartz, and muscovite at proportions of 22.3%, 69.9%, and 7.8%, respectively. The XRD analysis revealed the presence of quartz, kaolinite, and muscovite in the soil samples, accounting for approximately 69.9%, 22.3%, and 7.8%, respectively.

#### 2.1.2 Fly ash (FA)

In this study, FA is from the Duyen Hai 3 coal power plant in Vietnam. FA particles are spherical, ranging from 0.5 to 55  $\mu\text{m}$ , mostly smaller than 20  $\mu\text{m}$  (Fig. 1). The specific gravity of FA was 2.44 according to ASTM C188-25 [14]. X-ray diffraction (XRD) analysis showed  $\text{SiO}_2$ ,  $\text{Al}_2\text{O}_3$ , and  $\text{Fe}_2\text{O}_3$  content at 83.65%, exceeding the 70% threshold required in the ASTM C618-25a [15]. This FA is class F and suitable for the creation of geopolymers.

**Table 1** Basic properties of the soil used

Properties	Results	Test method
Sand content (%)	25.45	ASTM D6913/D6913M-17 [8]
Silt content (%)	37.86	ASTM D6913/D6913M-17 [8]
Clay content (%)	36.69	ASTM D6913/D6913M-17 [8]
Specific gravity	2.66	ASTM D854-23 [9]
Liquid limit, LL (%)	36.5	ASTM D4318-17e1 [10]
Plastic limit, PL (%)	19.6	ASTM D4318-17e1 [10]
Plasticity index, PI (%)	16.9	ASTM D4318-17e1 [10]
Optimum water content (%)	12.10	ASTM D1557-12(2021) [11]
Maximum dry unit weight (kN/m <sup>3</sup> )	1.924	ASTM D1557-12(2021) [11]

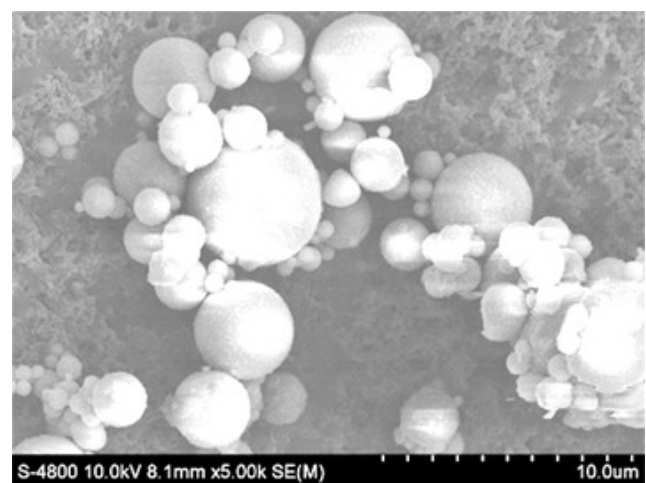


**Fig. 1** SEM image of fly ash at 5,000× magnification

### 2.1.3 Alkaline activator solution

In this work, alkaline activator solutions (AAS) consisting of sodium silicate ( $\text{Na}_2\text{SiO}_3$ ) and sodium hydroxide (NaOH) were utilized. Both  $\text{Na}_2\text{SiO}_3$  and NaOH were obtained from a local company. The sodium silicate, in liquid form, contained 19.3%  $\text{Na}_2\text{O}$ , 20.5%  $\text{SiO}_2$ , and 60.2% water, provided by the supplier. The specific gravity of SH was determined to be  $2.13 \text{ g/cm}^3$ , while the specific gravity of  $\text{Na}_2\text{SiO}_3$  was found to be  $1.44 \text{ g/cm}^3$ . The NaOH was in pellet form with a purity of 97% and a diameter of 3 mm.

Past studies have indicated that the molar concentration of NaOH plays a vital role in the mechanical and durability properties of geopolymer-stabilized materials [16]. It has been reported in the literature [17, 18] that the molar concentration of SH typically falls within the range of 4 M to 20 M and positively affects the strength of geopolymer-stabilized materials. Considering the economic aspect and the findings from previous studies [19], this work employed a 10 M SH concentration. As reported by Hardjito and Rangan [20], the 1 kg production of 10 M SH solution required 314 g of SH in solid form. Regarding the alkaline activator solution-to-fly ash (AAS/FA) ratio, a ratio of 0.4 was used in previous publications [21, 22].

## 2.2 Experiment

### 2.2.1 Sample preparation and mix proportion

In this study, natural soil was subjected to a series of preparation steps. Initially, the soil was dried at a temperature of  $55 \text{ }^\circ\text{C}$  for 12 h. Following this, the natural soil was crushed to separate the grain particles. Then, the soil was sieved at 4.0 mm for further analysis and testing. The modified Proctor compaction test was performed on samples of 152.4 mm diameter  $\times$  116.4 mm height (4.54 kg hammer, 5 layers, 56 hammer blows per layer) to determine optimum manufacturing moisture content and the corresponding maximum dry density, which simulated the in-situ rammed earth [23]. The preselected dry density of the GSCE sample was  $1.95 \text{ kN/m}^3$  for all samples, based on the laboratory compaction test. Each sample was prepared with a mass of 330 g of soil, 100 g of FA, and 40 g of NaOH and  $\text{Na}_2\text{SiO}_3$  solution. When the  $\text{Na}_2\text{SiO}_3/\text{NaOH}$  ratio is increased from 1.0 to 2.0, with constant ratios of AAS/FA at 0.4 and FA/Soil at 0.3. This range was selected based on previous studies showing that silicate-to-hydroxide ratios between 1.0 and 2.0 promote optimal geopolymerization kinetics and mechanical performance while avoiding excessive viscosity or premature gelation. Ratios within this window are commonly reported for alkali-activated

systems intended for structural and environmental applications [24]. The selected range, therefore, represents a balance between workability and reaction efficiency under practical conditions.

The samples for unconfined compression tests were manufactured in cylindrical steel molds with an inner diameter of 5 cm and a height of 10 cm. The molds were filled in three layers following the specifications of the ASTM D2166/D2166M-24 [25]. The samples were produced in two series. In the first series, the samples were prepared using different combinations of  $\text{Na}_2\text{SiO}_3/\text{NaOH}$  ratios and temperature conditions: room temperature,  $60 \text{ }^\circ\text{C}$  and  $90 \text{ }^\circ\text{C}$  for 24 h. The curing ages were 7, 14, 28, 35, 90, and 180 days. The purpose was to evaluate the compressive strength of the GSCE under these varied conditions. In the second series, the selected samples with various  $\text{Na}_2\text{SiO}_3/\text{NaOH}$  ratios cured at  $90 \text{ }^\circ\text{C}$  and 14 days were submerged in different solutions, following the guidelines specified in ASTM D559/D559M-15(2023)e1 [26]. This condition allows meaningful comparison with existing literature and provides insight into early-stage reaction mechanisms relevant to field curing scenarios with thermal assistance [27].

The issue of saline and acidic soils in Vietnam, particularly in the Mekong River Delta (MRD), is a significant concern that can be exacerbated by climate change impacts, such as sea level rise and salinity intrusion [28]. These environmental changes can adversely affect agricultural soils and soils used for construction materials, including soil stabilization and rammed earth (RE) walls. In fact, salinity intrusion in the MRD of Vietnam, which is associated with low water discharge from upstream, has worsened due to El Niño events and drought. Results of the research revealed that the pH range of soil decreased from 5.14–5.72 to 4.08–5.14 when the soil salinity increased from 0 to 2.5% [28]. In that context, the GSCE sample is expected to simulate the environmental conditions of the study area in which salt water or acid water impacts the samples throughout usage. Three types of solutions are tap water, salt water with concentrations of 0.725 g/L, and an acid solution with pH = 4. A salt solution with a concentration of 0.725 g/L was prepared by dissolving 0.725 g of NaCl (96% purity) in one liter of distilled water. This concentration corresponds to the salinity determined from analyses of groundwater samples collected at a geological borehole in Nha Be, Ho Chi Minh City, Vietnam. The acidic pH = 4 was chosen to represent mildly aggressive environmental conditions commonly encountered in

acid rain exposure, contaminated groundwater, or soil–material interactions. In addition, past publications [23] indicated that the wetting-drying (w-d) cycle test is usually conducted within 12 cycles with the target cycles of 1, 3, 6, 9, and 12. The chosen 12 cycles simulated the repeating flooding in Vietnam [29].

### 2.2.2 Test procedure

#### Unconfined compressive strength (UCS)

The UCS was determined following ASTM D4219-22 [30]. The axial strain rate is usually 0.5–1.0% per minute. A 1.0 mm/min axial strain rate (corresponding to 1.0% per minute) was applied in the present study. The UCS value was determined by dividing the maximum load by its cross-sectional area. The maximum load represents the peak point that occurs under the compressive force. The reported results, the average of three test samples, are common practice in experimental testing and analysis.

#### Wetting-drying cycle test

The strength of the geopolymer material significantly improved at a short-term curing age. Thus, this study used samples cured for 14 days that consisted of 12 w-d cycles. The w-d cycle procedures involved several steps. Initially, the samples were submerged in a predetermined solution at room temperature for 5 h to ensure saturation. After

immersion, the samples were removed and placed in a 70 °C oven for 42 h to simulate the drying phase. Subsequently, the samples were air-dried at room temperature for 1 h to facilitate drying further. The w-d cycles were performed for a specific number of cycles, ranging from 1 to 12, with steps of 1, 3, 6, 9, and 12. Fresh solutions were used for each cycle, requiring replacement before immersing the samples again. Finally, the UCS of the samples was determined to assess the strength behavior of the GSCE after undergoing the w-d cycling process. A typical summary procedure of w-d cycles is presented in Fig. 2.

#### Advanced technique analysis

X-ray diffraction is a technique to determine the amorphous and crystalline components in the sample. This work uses the JSM-IT 200 instrument manufactured by JEOL. Besides, the FTIR technique was performed using the Nicolet™ iS50 FTIR Spectrometer, which is utilized to examine the chemical bonds and functional groups in the tested sample. Fig. 3 summarizes the detailed process of this study.

## 3 Results and discussion

### 3.1 Stress-strain relationship of GSCE

Fig. 4 illustrates the stress-strain relationships of GSCE at different curing ages. The curing ages tested were 7, 14, 28, 56, 90, and 180 days, and the samples were prepared



Fig. 2 Procedure of preparing w-d cycles

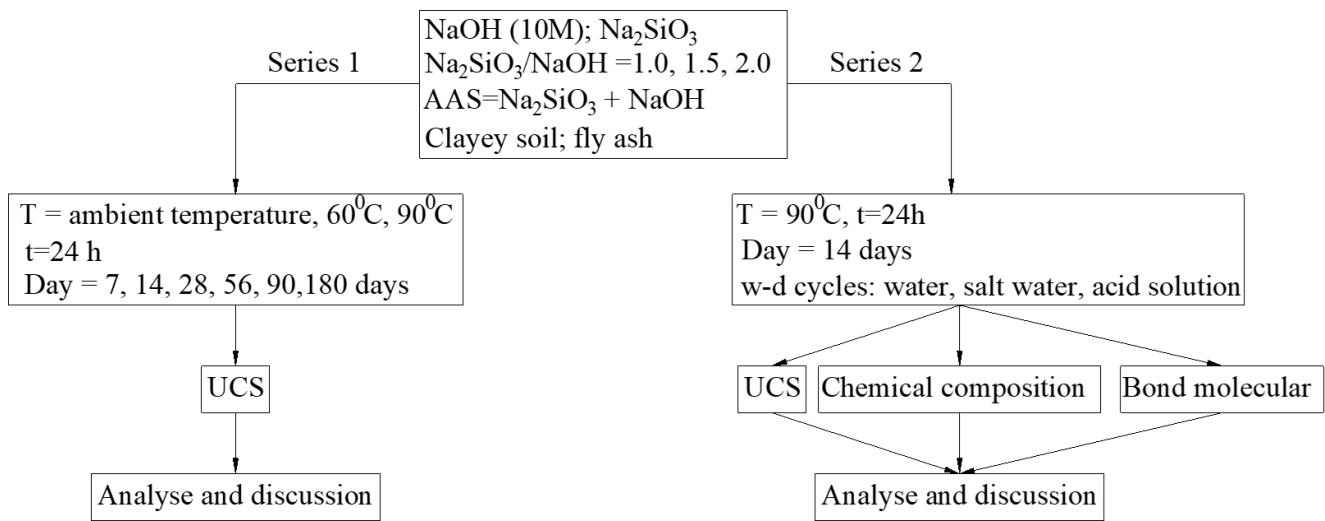


Fig. 3 Flow chart of this study

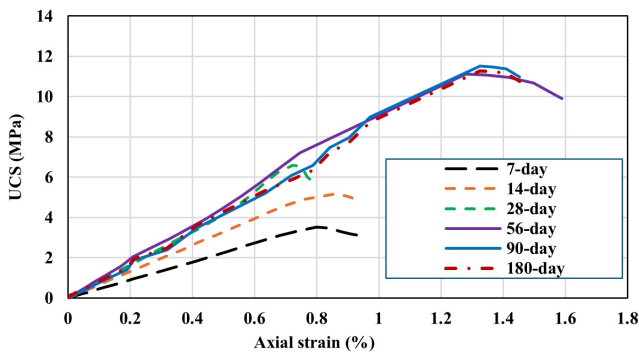


Fig. 4 Typical stress-strain relationships of GSCE, cured at ambient temperature ( $\text{Na}_2\text{SiO}_3/\text{NaOH} = 1.5$ )

with a  $\text{Na}_2\text{SiO}_3/\text{NaOH} = 1.5$  and cured at ambient temperature. Other results prepared at  $\text{Na}_2\text{SiO}_3/\text{NaOH} = 1.0$  and  $2.0$  are not presented due to the same behaviors. In analyzing the data plotted in Fig. 4, it is observed that the axial strain does not exhibit a specific trend. Obtained strain inhomogeneity may be due to measurement over the entire length of the specimen. For instance, when the curing age increases from 7 to 28 days, the axial strains obtained at the peak stress range from 0.70 to 0.85. However, with a further increase in curing time to 56–180 days, the strain at peak stress increases to approximately 1.3%. The strain gradually decreases after reaching peak stress, except for the 28-day curing period without residual stress. The result indicated that the sample described ductile behavior in the long term. The findings of this study are in agreement with a previous publication by Abdullah et al. [31], who investigated the compressive strength of soil treated with 10%–20% geopolymer; however, in their results, a ductile response was obtained at 7 days for 10% geopolymer stabilized soil. The stress-strain behavior of the GSCE samples in this study is attributed to the formation of N-A-S-H

(sodium-aluminum-silicate-hydrate) and C-A-S-H (calcium-aluminum-silicate-hydrate) products, which create linkages between soil particles [32]. Advanced techniques were employed and discussed in Sections 3.6–3.7 to investigate this behavior further.

### 3.2 Effect of curing time on compressive strength

Fig. 5 shows the compressive strength of GSCE with a curing period of 7, 14, 28, 56, 90, and 180 days in the case of  $\text{Na}_2\text{SiO}_3/\text{NaOH} = 1.0, 1.5,$  and  $2.0$ . The samples were cured at ambient temperature. In general, the compressive strength of GSCE increases with longer curing time. This observation is a common trend observed in geopolymer matrices, where the chemical reactions continue to enhance their strength over time. Short-term curing, such as 14 days, resulted in significant development of strength. At 14 days, the compressive strength values ranged from 5.2–6.3 MPa for different  $\text{Na}_2\text{SiO}_3/\text{NaOH}$  ratios, which satisfied the construction building material ( $> 2.8$  MPa, according to British Standard 5628-1:2005 [33]). Similarly, at 56 days of curing, the UCS values range from 6.98–10.38 MPa for different

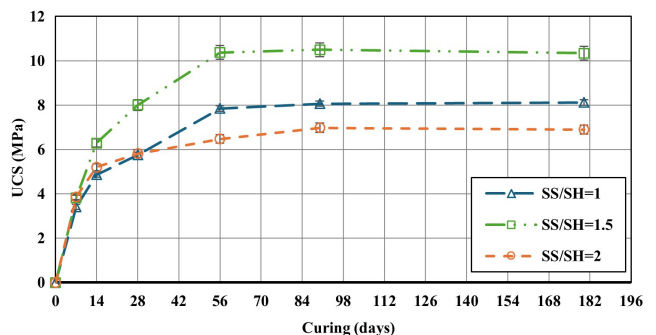


Fig. 5 Development of strength in functions of the curing time (at ambient temperature)

$\text{Na}_2\text{SiO}_3/\text{NaOH}$  ratios. However, at longer curing ages, the compressive strength slowly decreases. This decrease occurs regardless of the  $\text{Na}_2\text{SiO}_3/\text{NaOH}$  ratios. The specific UCS values at this stage are not mentioned. The findings from Zhou et al. [34] investigated ground-granulated blast furnace slag-GSCE and reported a similar trend of decreasing compressive strength beyond 120 days of curing. Peng et al. [35] explained this reduction in strength. They attributed it to dry shrinkage, which leads to internal stress and the formation of shrinkage cracks in the GSCE samples. It is noted that the geopolymer-stabilized soil has a higher strength compared to cement-stabilized soil, as presented in previous publications [13].

### 3.3 Effect of $\text{Na}_2\text{SiO}_3/\text{NaOH}$ ratios on compressive strength

It is noted that the relationship between the  $\text{Na}_2\text{SiO}_3/\text{NaOH}$  ratio and compressive strength may vary depending on the specific characteristics of the soil, such as its mineralogy, plasticity, and pore structure. To obtain accurate and reliable results, it is advisable to conduct laboratory tests on soil samples at different  $\text{Na}_2\text{SiO}_3/\text{NaOH}$  ratios to determine the specific behavior of the GSCE. Fig. 6 presents the variation in UCS of GSCE with different  $\text{Na}_2\text{SiO}_3/\text{NaOH}$  ratios. The tests included samples with  $\text{Na}_2\text{SiO}_3/\text{NaOH}$  ratios of 1.0, 1.5, and 2.0, at ambient temperature. Notably, GSCE samples prepared with a  $\text{Na}_2\text{SiO}_3/\text{NaOH}$  ratio of 1.5 exhibited a significant increase in compressive strength compared to those with ratios of 1.0 and 2.0. The UCS values for the  $\text{Na}_2\text{SiO}_3/\text{NaOH} = 1.5$  samples were 1.1–1.6 times higher, depending on the curing duration, except for the 7-day curing period. This optimal  $\text{Na}_2\text{SiO}_3/\text{NaOH}$  ratio of 1.5 was consistent with the findings of Pavithra et al. [36]. The specific reasons for the superior strength at the  $\text{Na}_2\text{SiO}_3/\text{NaOH}$  ratio of 1.5 should be explicitly mentioned in the provided information. However, this ratio is believed to achieve an optimal balance for the geopolymerization

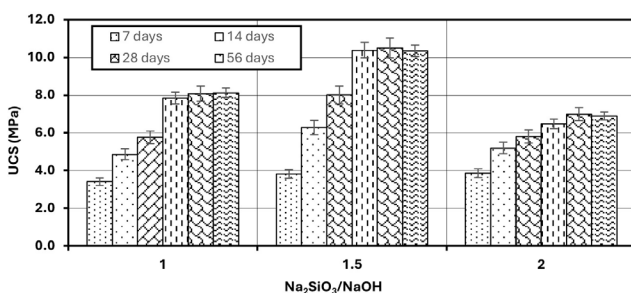


Fig. 6 Effects of  $\text{Na}_2\text{SiO}_3/\text{NaOH}$  ratios on compressive strength at ambient temperature

process, leading to enhanced strength in GSCE. The standard deviations, as indicated by the error bars, are relatively small, generally within approximately 5–10% of the mean UCS values, demonstrating good repeatability of the test results. Slightly larger variations are observed at higher strength levels, particularly for the  $\text{Na}_2\text{SiO}_3/\text{NaOH}$  ratio of 1.5 at 28 and 56 days, which may be attributed to minor heterogeneity in geopolymer gel formation and specimen preparation. Overall, the limited standard deviations confirm the reliability of the experimental data and indicate that the observed strength differences are governed primarily by activator ratio and curing age rather than experimental uncertainty. A more comprehensive explanation and investigation will be presented in the FTIR section.

### 3.4 Effect of the curing temperature on the compressive strength

Fig. 7 illustrates the typical compressive strength of GSCE with various  $\text{Na}_2\text{SiO}_3/\text{NaOH}$  ratios of 1 under three temperature conditions: ambient temperature, 60 °C, and 90 °C during the initial 24 h. The data in Fig. 7 shows that the compressive strength of GSCE increased with higher curing temperatures. The improvement in strength was particularly significant at 7, 14, and 56 days. For curing of 56 and 90 days, the strength results were turbulent at 60 °C. This inconsistency might be attributed to issues during sample production or problems with the oven used for elevated-temperature curing. Shihab et al. [37] also observed that curing 90 °C for 24 h significantly improved the compressive strength, which was similar to the current study. Their research indicated that the maximum peak strength was achieved with a  $(\text{Na}_2\text{SiO}_3 + \text{NaOH})/\text{FA}$  ratio of 3.8 at 90 °C for 24 h. On the other hand, certain studies [38] have suggested that the recommended heat-curing regime for optimal performance and energy efficiency in geopolymer concrete is 75 °C for 18 h.

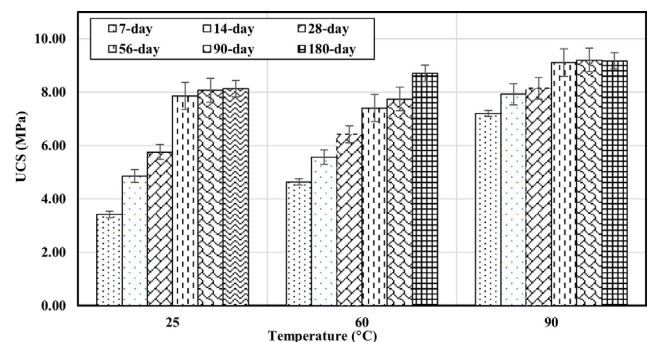


Fig. 7 UCS cured in room temperature curing,  $\text{Na}_2\text{SiO}_3/\text{NaOH} = 1.0$

### 3.5 Effect of w-d cycles on the durability of GSCE with various solutions

As mentioned above, for temperature curing at 90 °C, the compressive strength developed mainly at 14 days of curing. In addition, the strength at 14 days can reach the target strength in civil engineering materials, as indicated in Section 3.2. Thus, the experiment hereafter was conducted on samples cured at 90 °C for 24 h, then cured at room temperature for 14 days. A series of w-d cycles was tested to investigate the compressive strength of GSCE after w-d cycles. Tap water, a pH = 4 solution, and a 0.725 g/L salt solution were used in this testing process. The number of cycles tested was denoted as C = 1, 3, 6, 9, and 12. As depicted in Fig. 8, the compressive strength of GSCE diminishes with an increase in the number of w-d cycles. This observation signifies the substantial influence of w-d cycles on the strength of GSCE. The range of compressive strength values after the w-d cycles was recorded as follows (in MPa): 6.23–8.7 (C = 1 cycles), 5.73–8.03 (C = 3 cycles), 4.97–7.37 (C = 6 cycles), 4.20–7.17 (C = 9 cycles), and 3.75–6.29 (C = 12 cycles). When considering different Na<sub>2</sub>SiO<sub>3</sub>/NaOH ratios, the decrease in strength after 12 w-d cycles was found to be 49.93% for Na<sub>2</sub>SiO<sub>3</sub>/NaOH = 1.0, 29.88% for Na<sub>2</sub>SiO<sub>3</sub>/NaOH = 1.5, and 48.74% for Na<sub>2</sub>SiO<sub>3</sub>/NaOH = 2.0, compared to the reference sample. The findings from this work are consistent with those of past studies by Kamaruddin et al. [39], who investigated geopolymer-modified coir fiber-reinforced stabilized marine clay, and Batista dos Santos et al. [40], who used a geopolymer composite reinforced with sisal fiber after 10 w-d cycles. The reduction in strength after a certain number of w-d cycles could be due to the loosening of cementation in GSCE over time. As the number of cycles increases, water absorption increases, causing the dissolution of precipitates in the cemented soil [41]. In general, the reduction of the mechanical property significantly depends on the cementation ability of the additive used.

Fig. 9 shows a fluctuation in the compressive strength of GSCE. The strength values of GSCE are in a range

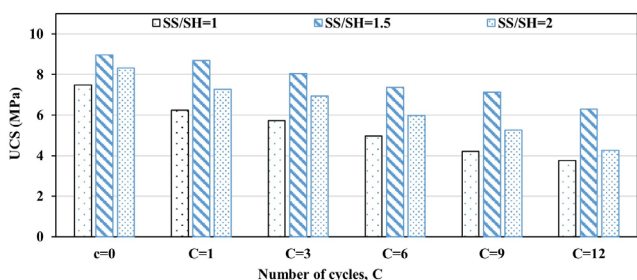


Fig. 8 Various compressive strengths with tap water

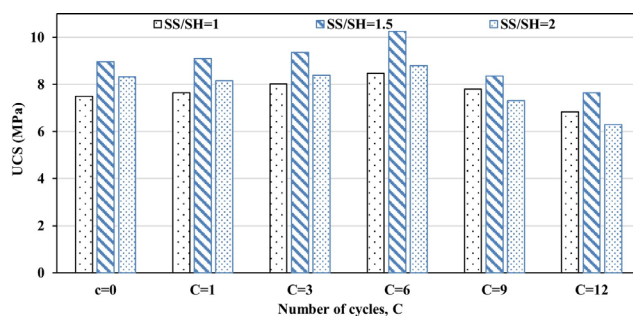


Fig. 9 Compressive strengths with pH = 4 solution

of 7.65–9.1 MPa, 8.02–9.35 MP, 8.47–10.25 MPa, 7.30–8.35 MPa, 6.30–7.65 MPa, respectively, for C = 1, 3, 6, 9, 12 cycles. An interesting result was obtained from this work, that the growth of cementitious products is dominant within the initial stage, C < 6; after that, the sample deterioration is dominant and causes the UCS reduction with C > 6. This phenomenon is consistent with the findings reported by Hoy et al. [42], who studied the durability of recycled asphalt pavement-fly ash geopolymer after submerging the sample at specific w-d cycles. The observed increase in UCS during the first three cycles (C = 1, 3, and 6) is likely attributed to the formation and contribution of calcium silicate hydrate (C-S-H) during the w-d process, as explained by certain studies [43]. When w-d cycles increase to 9, 12, the sample deterioration related to the decalcification of C-S-H may be the reason for reducing the strength of GSCE [44]. The XRD and FTIR techniques in Sections 3.6–3.7 will discuss and analyze more details about the increase in strength in the 3 first 3 w-d cycles.

Fig. 10 illustrates the compressive strengths of samples subjected to different w-d cycles in the presence of a 0.725 g/L salt solution. Similar to tap water observations, the strength of the samples decreases as the number of w-d cycles increases. Notably, the decline in strength is particularly pronounced at C = 9 and 12. Comparatively, after 12 w-d cycles, the strength decreases by 51.13%, 32.89%, and 48.98% for Na<sub>2</sub>SiO<sub>3</sub>/NaOH ratios of 1.0, 1.5, and 2.0, respectively, in comparison to the reference sample at the same Na<sub>2</sub>SiO<sub>3</sub>/NaOH ratio. For instance, the compressive

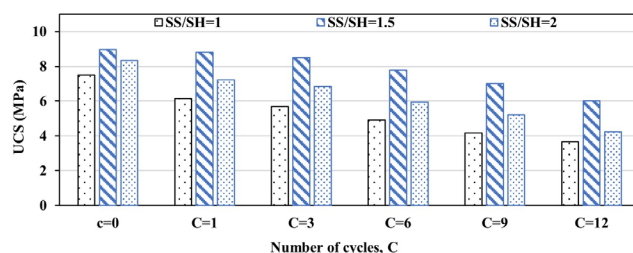


Fig. 10 Compressive strengths with 0.725 g/L salt solution

strength of GSCE is in a range of 3.66–7.49 MPa, 6.02–8.97 MPa, and 4.25–8.33 MPa, respectively, for  $\text{Na}_2\text{SiO}_3/\text{NaOH} = 1.0, 1.5, 2.0$ , after 12 w-d cycles.

### 3.6 XRD results

As presented in Section 3.4, when w-d cycles increased, the compressive strength decreased when submerged in tap water and salt water. Furthermore, with a pH = 4 acid solution, there are two special problems: the sample strength increases to  $C = 6$ , and  $\text{Na}_2\text{SiO}_3/\text{NaOH} = 1.5$  has the highest strength among the other ratios. Thus, the XRD technique determines whether chemical components are present in different forms across different types of samples. Typical samples are chosen to test in the XRD test, as indicated in Figs. 11–15, to investigate the changes in chemical composition. The results describe the typical mineral components found in samples, varying percentages, including Quartz, Muscovite, Kaolinite, Clinocllore, Hematite, and Gottardiite.

The data depicted in Fig. 16 shows that the obtained crystalline phase is predominant when the tested samples are in a pH = 4 acid solution, regardless of whether various  $\text{Na}_2\text{SiO}_3/\text{NaOH}$  solutions are used. In addition, samples prepared with  $\text{Na}_2\text{SiO}_3/\text{NaOH} = 1.5$  have a crystalline phase of 54.42%, which is remarkably more significant than those of other  $\text{Na}_2\text{SiO}_3/\text{NaOH}$  ratios. The XRD

results suggest that the increase in crystalline phases may have contributed to the strength enhancement observed in Sections 3.1–3.5. Alternatively, the change in strength can also be explained based on the findings of Ayub and Khan [45], who claimed that the improvement in strength was due to the changes in amorphous.

### 3.7 FTIR results

As in the session mentioned above, the sample containing  $\text{Na}_2\text{SiO}_3/\text{NaOH} = 1.5$  gives the greatest compressive value. In this part, an in-depth experiment was conducted to evaluate the reason causing the greatest value in compressive strength. The FTIR results of samples with various  $\text{Na}_2\text{SiO}_3/\text{NaOH} = 1.0, 1.5, 2.0$  ratios and w-d cycles are presented in Figs. 13 and 14. The spectrum of  $\text{Na}_2\text{SiO}_3$  shows the original connection before the geopolymerization process. Results show certain strong peaks at wavenumbers of around  $2800\text{ cm}^{-1}$  to  $3600\text{ cm}^{-1}$ ,  $2300\text{ cm}^{-1}$ ,  $1660\text{ cm}^{-1}$ ,  $1120\text{ cm}^{-1}$ ,  $1000\text{ cm}^{-1}$ ,  $900\text{ cm}^{-1}$ ,  $780\text{ cm}^{-1}$ ,  $650\text{ cm}^{-1}$ ,  $460\text{ cm}^{-1}$ . Fig. 17 shows the transmittance-wavenumber curve for samples cured 14 days without w-d cycles. Typical chemical bonds were shown as C-H at  $2900\text{ cm}^{-1}$  [46], constitutional water at  $1640\text{ cm}^{-1}$ ; and O-Si-O connection at  $800\text{ cm}^{-1}$  for the sample prepared with  $\text{Na}_2\text{SiO}_3/\text{NaOH} = 1$ ,  $\text{Na}_2\text{SiO}_3/\text{NaOH} = 1.5$ , and  $\text{Na}_2\text{SiO}_3/\text{NaOH} = 2.0$ . It has been proven that the  $\text{Na}_2\text{SiO}_3/\text{NaOH} = 1.5$  sample showed a clear

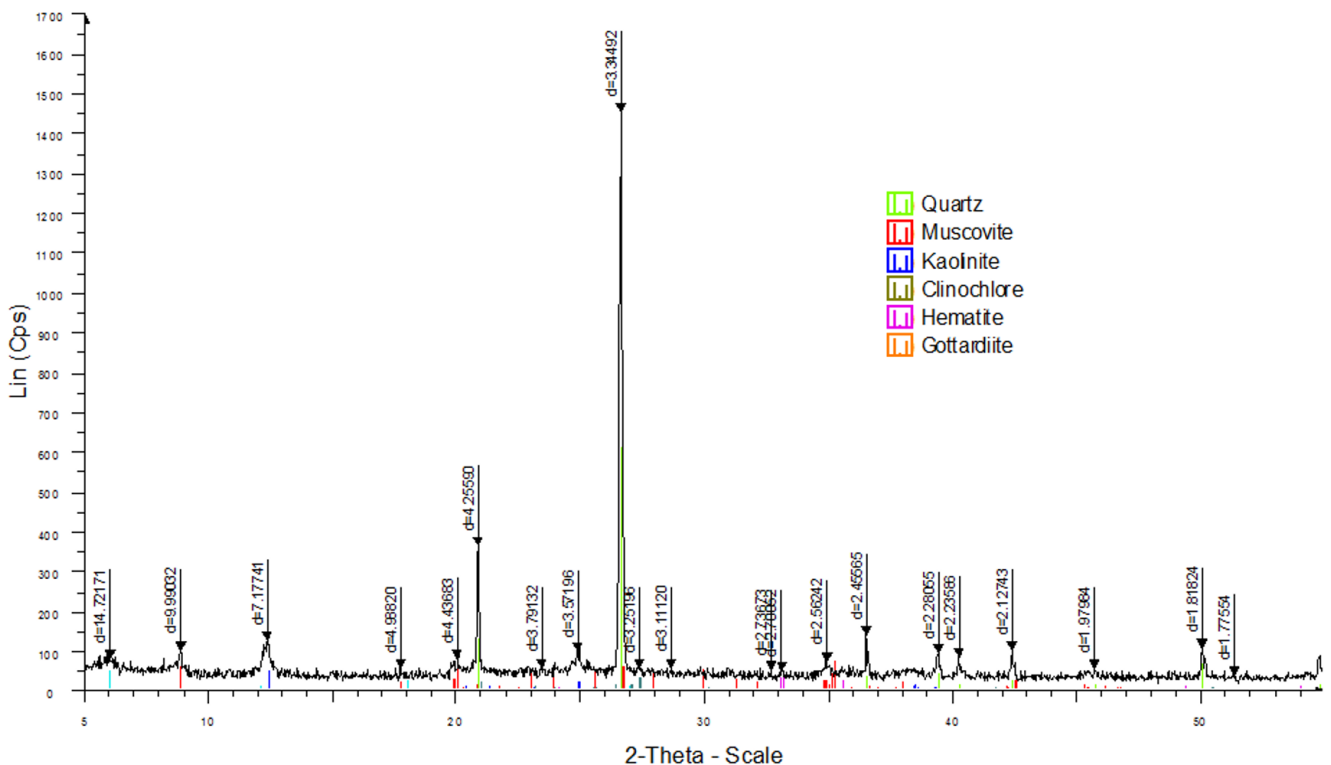


Fig. 11 XRD patterns of GSCE in various solutions if  $\text{Na}_2\text{SiO}_3/\text{NaOH} = 1$ , salt water of 0.725 g/L,  $C = 6$

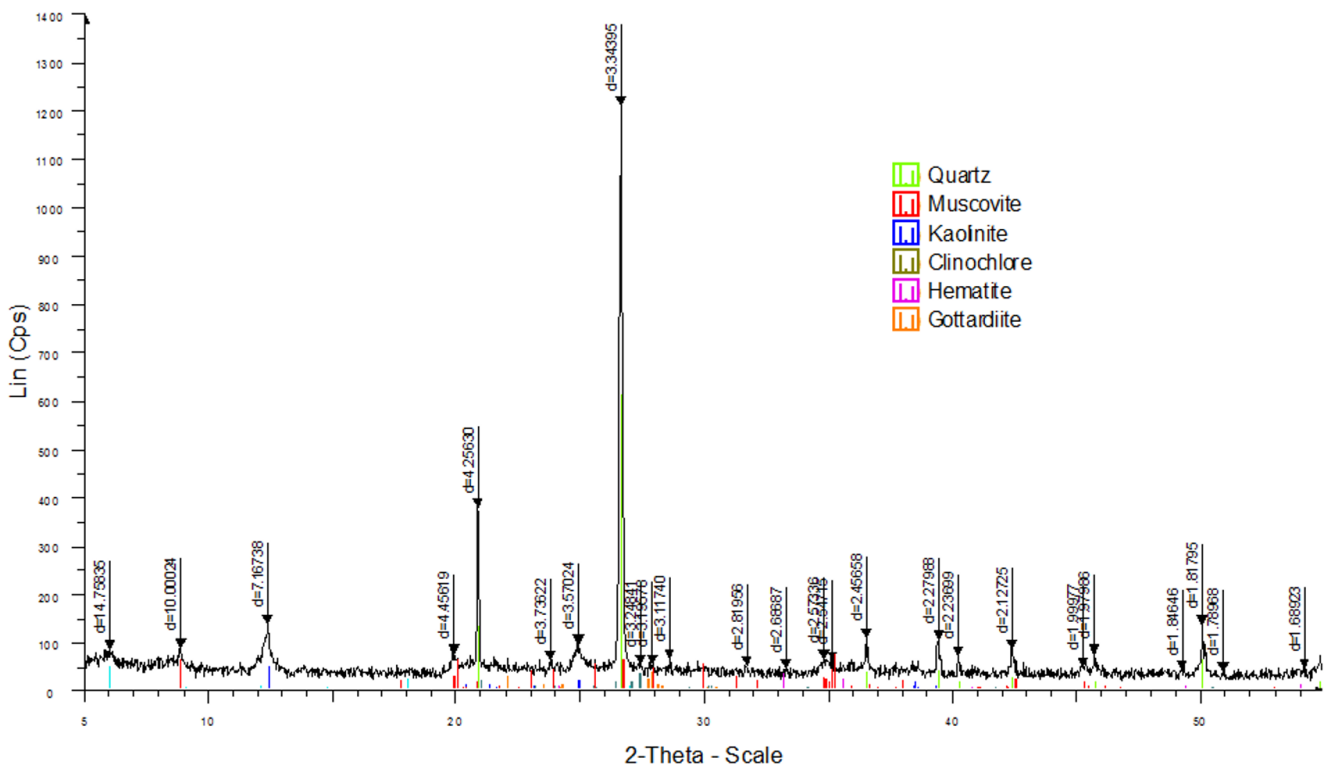


Fig. 12 XRD patterns of GSCE in various solutions if  $\text{Na}_2\text{SiO}_3/\text{NaOH} = 1$ ,  $\text{pH} = 4$ ,  $C = 6$

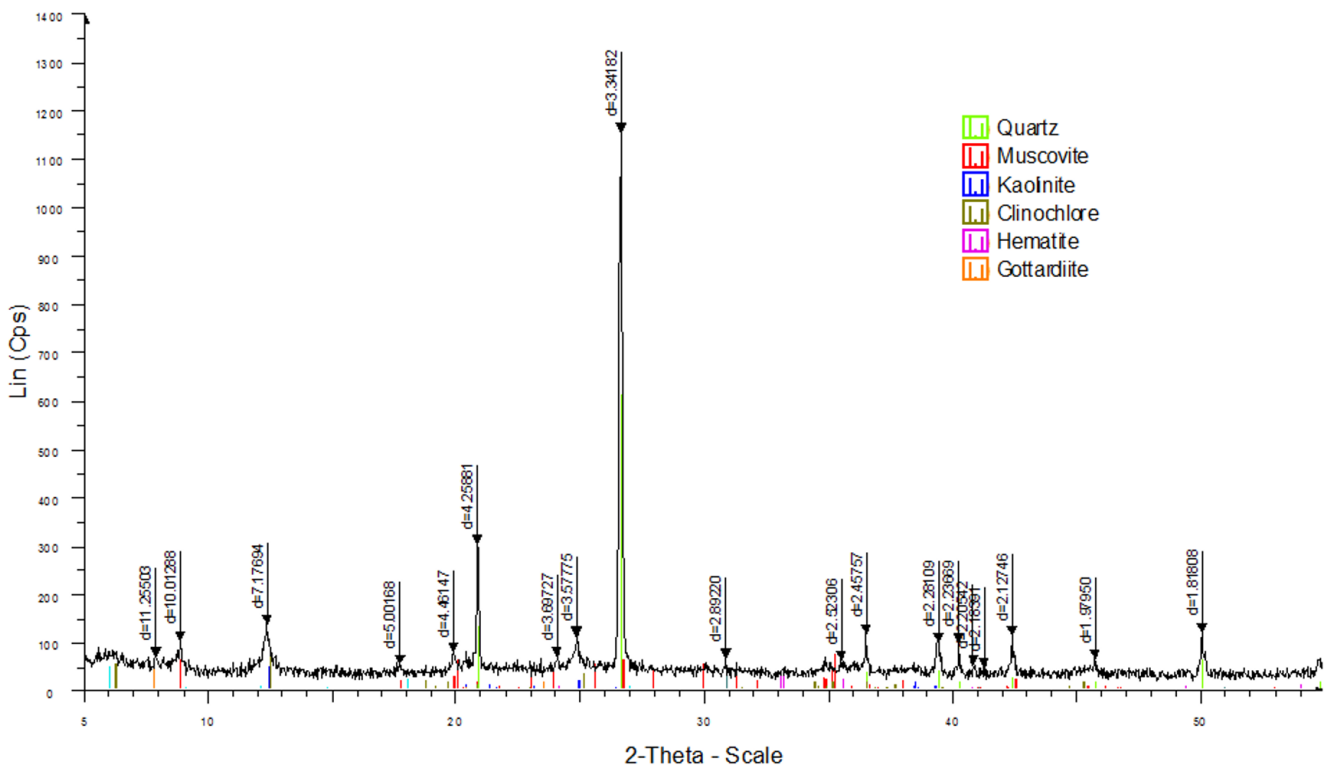


Fig. 13 XRD patterns of GSCE in various solutions if  $\text{Na}_2\text{SiO}_3/\text{NaOH} = 1.5$ ,  $\text{pH} = 4$ ,  $C = 6$

peak at a wavenumber of  $800\text{ cm}^{-1}$  compared to the two other samples, which may have caused the increase in compressive strength. Compared to pure  $\text{Na}_2\text{SiO}_3$ , all samples show the evolution of chemical bonds when the test sample is without w-d cycles.

With samples exposed to w-d cycles, Figs. 18–20 show the spectrum with wavenumbers for samples prepared with  $\text{Na}_2\text{SiO}_3/\text{NaOH} = 1, 1.5$ , and  $2.0$  at various typical w-d cycles in  $\text{pH} = 4$  solution. Clear bond connections, such as C-H, constitutional water, and O-Si-O bonds, are

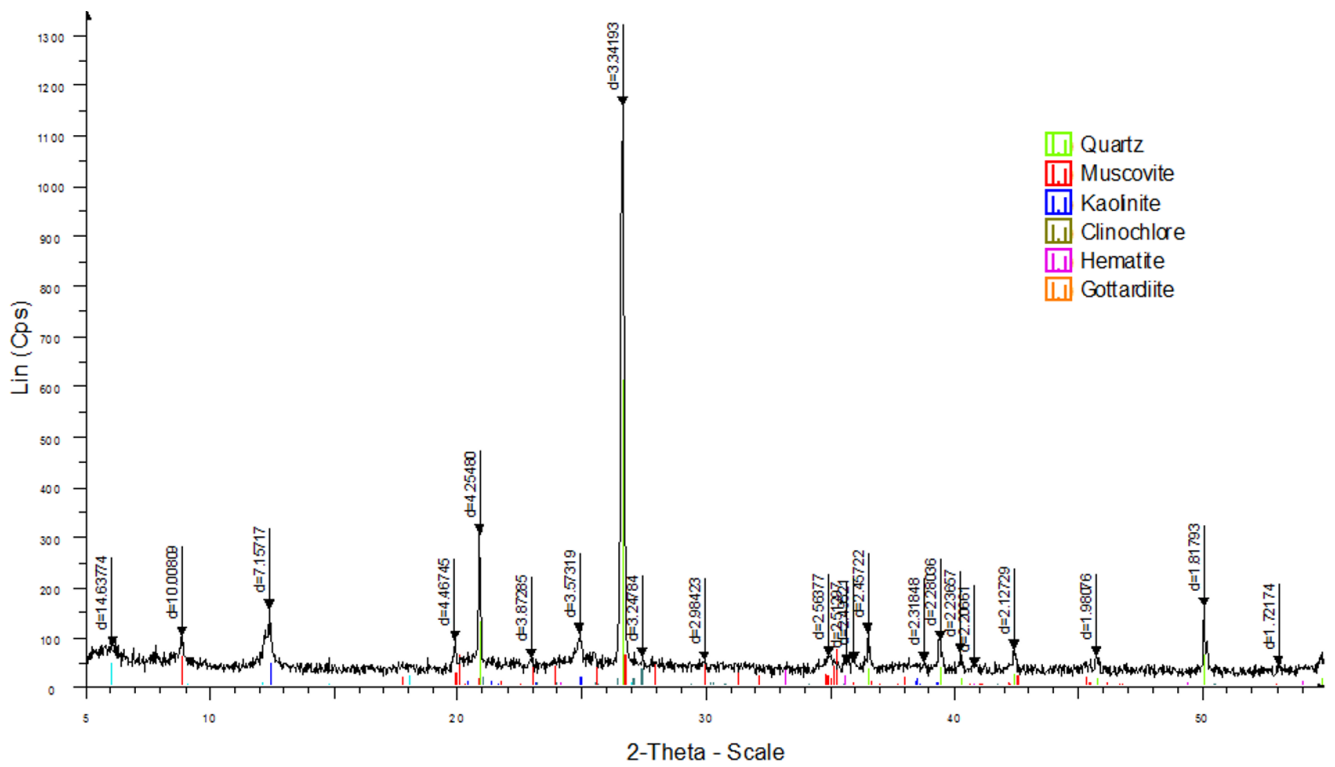


Fig. 14 XRD patterns of GSCE in various solutions if  $\text{Na}_2\text{SiO}_3/\text{NaOH} = 2.0$ , salt water of 0.725 g/L,  $C = 6$

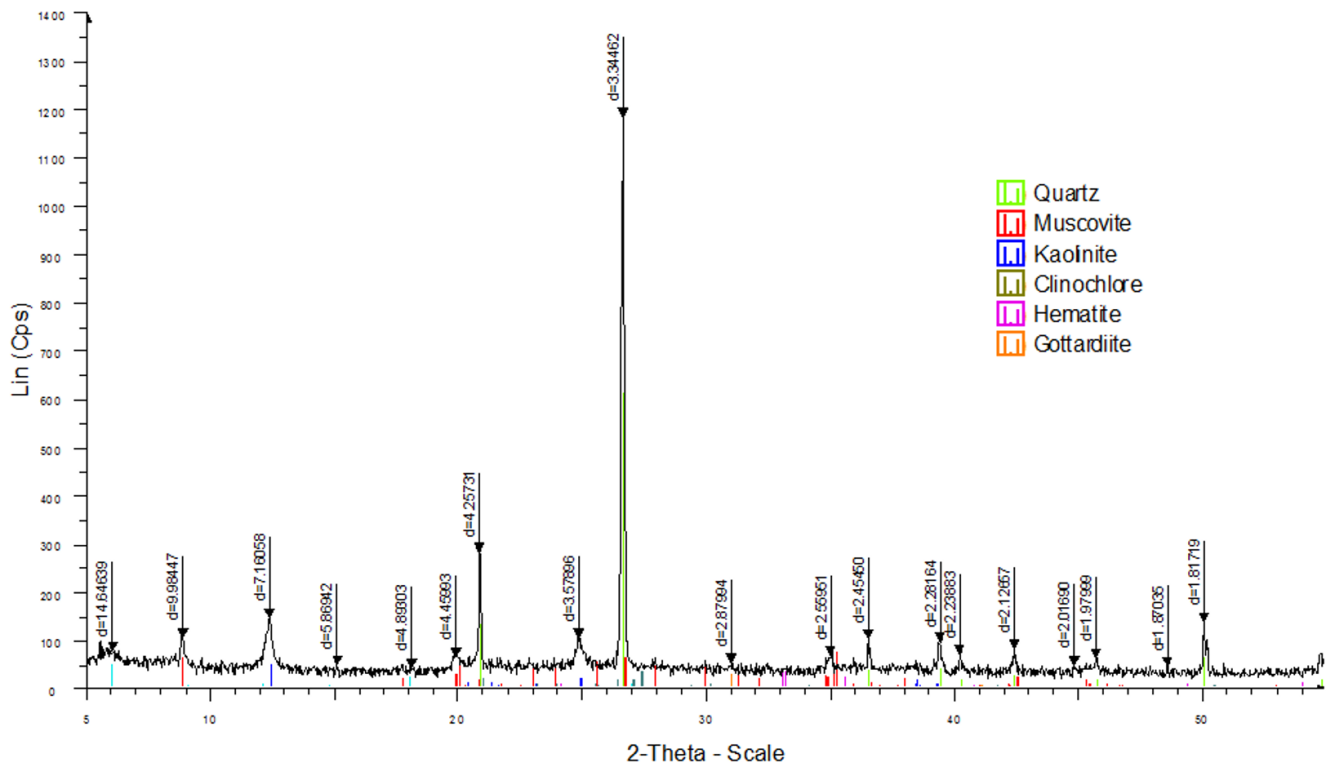


Fig. 15 XRD patterns of GSCE in various solutions if  $\text{Na}_2\text{SiO}_3/\text{NaOH} = 2.0$ ,  $\text{pH} = 4$ ,  $C = 6$

shown in these samples. It is recognized that at the same  $\text{Na}_2\text{SiO}_3/\text{NaOH}$  ratio, samples exposed to  $C = 6$  cycles show a strong reverse peak (at  $800\text{ cm}^{-1}$  and  $2900\text{ cm}^{-1}$ ) compared to samples tested in  $C = 1$  and  $C = 12$  cycles.

The higher peak indicates a stronger chemical bond in the sample, resulting in greater strength. The results obtained have clarified why sample  $C = 6$  exhibits higher intensity than the other samples.

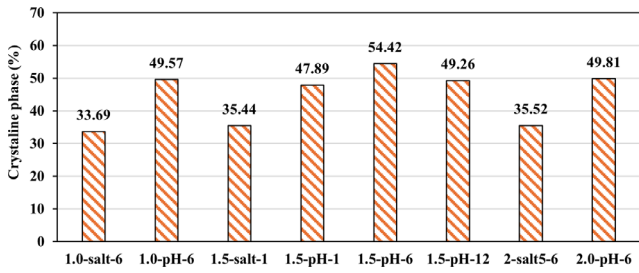


Fig. 16 Crystalline phase of GSCE in various solutions,  $\text{Na}_2\text{SiO}_3/\text{NaOH}$ , and cycles

Fig. 21 depicts the spectra of samples at  $C = 6$  cycles for varying  $\text{Na}_2\text{SiO}_3/\text{NaOH}$  ratios of 1.0, 1.5, and 2.0. It is noteworthy that the vibrations of O-Si-O bands and pseudo-crystal lattice vibrations are observed for all samples. However, the sample with  $\text{Na}_2\text{SiO}_3/\text{NaOH} = 1.5$  exhibits a peak transmittance percentage, indicating a strong molecular bond. Additionally, constitutional water is distinctly

detected at the wavenumber of  $1640\text{ cm}^{-1}$  for the  $\text{Na}_2\text{SiO}_3/\text{NaOH} = 1.5$  sample, while it remains unclear for  $\text{Na}_2\text{SiO}_3/\text{NaOH} = 1.0$  and 2.0 samples. Furthermore, the OH group and water stretching vibrations were also clearly observed at a wavenumber around  $3600\text{ cm}^{-1}$ , and the  $\text{Na}_2\text{SiO}_3/\text{NaOH} = 1.5$  sample showed the strongest transmittance at this wavenumber. At wave numbers of around  $1000\text{--}1010\text{ cm}^{-1}$ , Si-O-Si asymmetric stretching vibrations are found in all samples. The clear peak at  $1460$  of  $\text{Na}_2\text{SiO}_3/\text{NaOH} = 1.5$  also confirms the existence of a strong geopolymer in the sample [46]. The peaks at  $2900\text{ cm}^{-1}$  were more evident for the case of  $\text{pH} = 4, C = 6$ , especially than the others. Finally, the  $\text{Na}_2\text{SiO}_3/\text{NaOH} = 1.5$  sample shows a remarkable difference from the other samples in the  $3600\text{--}3900\text{ cm}^{-1}$  region. Based on the mechanical properties and durability of stabilized geopolymer soil obtained, XRD, and FTIR observations. In general,

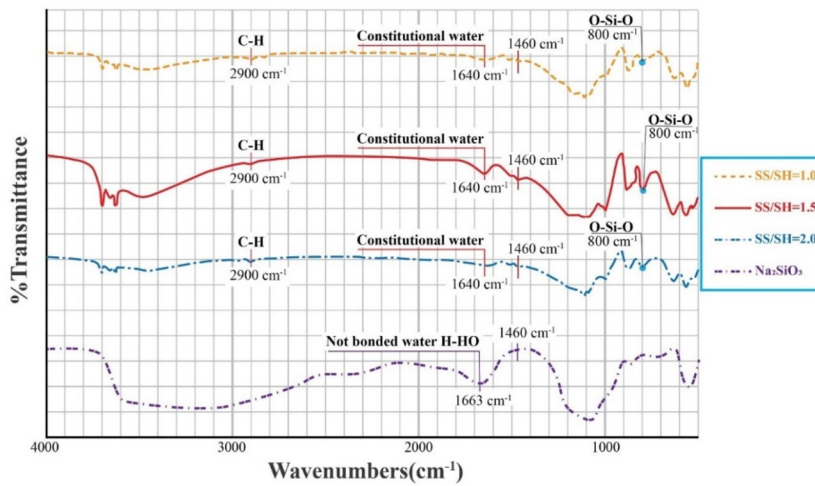


Fig. 17 FTIR test for reference samples

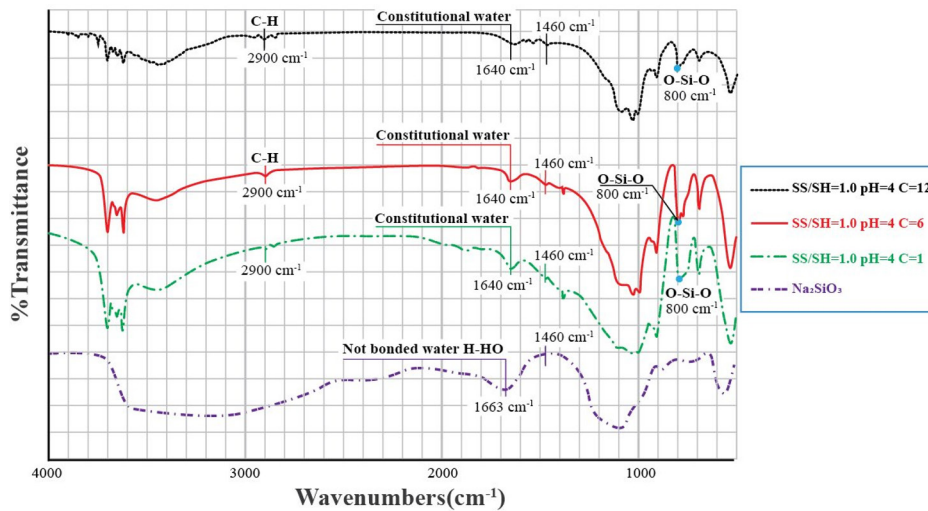


Fig. 18 FTIR test for samples exposed to w-d cycles of 1, 6, 12 at  $\text{Na}_2\text{SiO}_3/\text{NaOH} = 1.0$

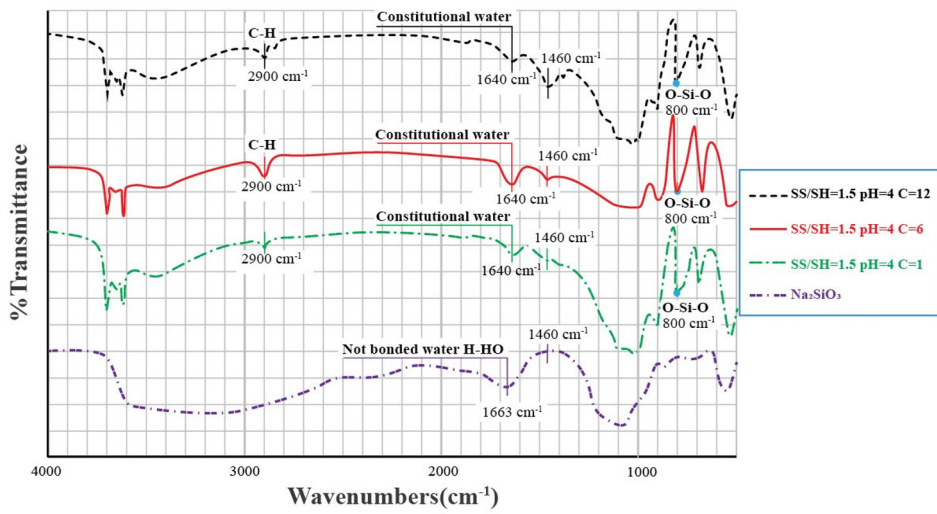


Fig. 19 FTIR test for samples exposed to w-d cycles of 1, 6, 12 at  $\text{Na}_2\text{SiO}_3/\text{NaOH} = 1.5$

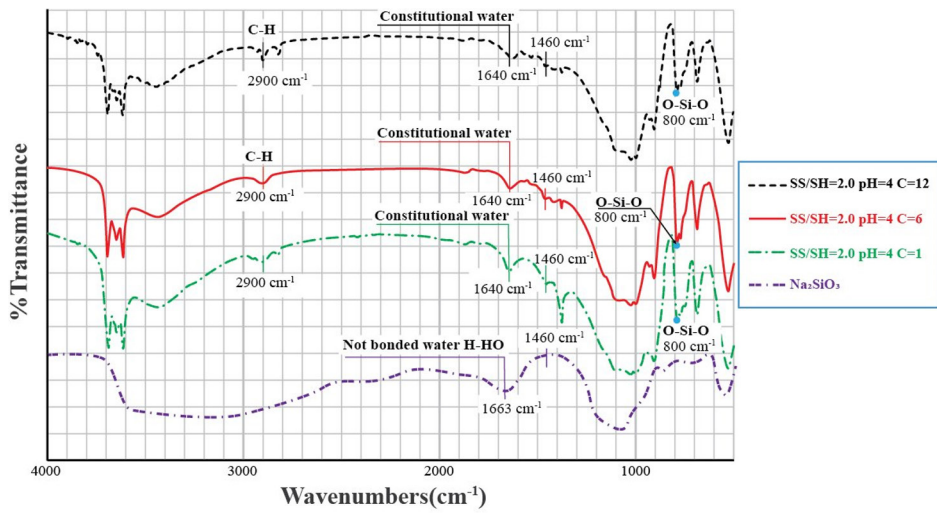


Fig. 20 FTIR test for samples exposed to w-d cycles of 1, 6, 12 at  $\text{Na}_2\text{SiO}_3/\text{NaOH} = 2.0$

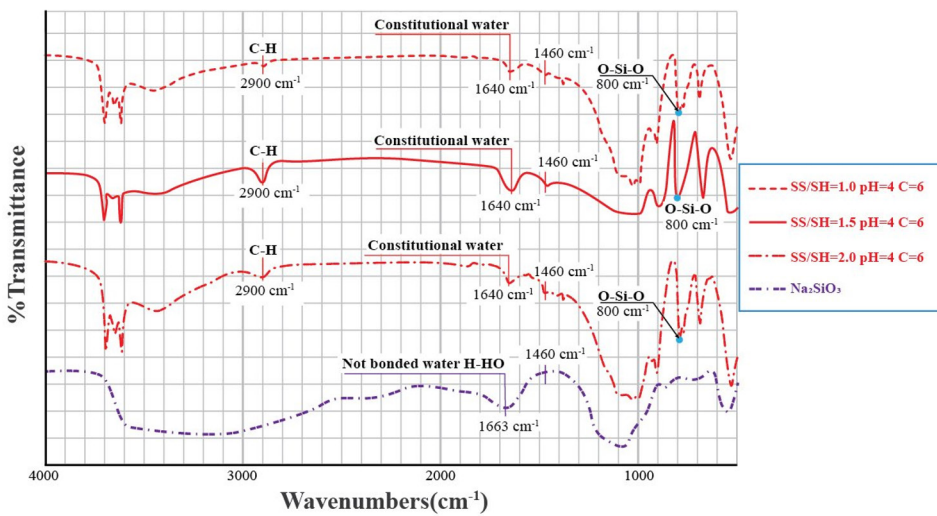


Fig. 21 FTIR test for samples exposed to C = 6 cycles

geopolymerization is a chemical process in which aluminosilicate-rich materials react with alkaline activators to form a durable inorganic binder. Under high-pH

conditions, the solid precursors dissolve, releasing silicate and aluminate species into solution. These species then rearrange and undergo polycondensation, forming

a three-dimensional aluminosilicate gel network (commonly N–A–S–H or related gels). The gel precipitates, fills pores, and binds unreacted particles. At long term, the gel densifies and hardens, leading to improved mechanical strength and long-term chemical and thermal stability.

#### 4 Conclusions

This paper investigates the mechanical properties and durability of geopolymer-stabilized compressed earth under various environmental conditions. The samples were subjected to different curing conditions, including curing time, temperature,  $\text{Na}_2\text{SiO}_3/\text{NaOH}$  ratios, wet–dry (w–d) cycles, and immersion solutions. Based on the data obtained, the following key conclusions can be drawn:

- The results showed that the strength of GSCE reaches more than 5.0 MPa after a 14-day curing period, which satisfies the existence of several standards. The best composition for the compressive strength was  $\text{Na}_2\text{SiO}_3/\text{NaOH} = 1.5$ , and the sample was cured at 90 °C for 24 h.
- When the number of wetting–drying cycles increases, the compressive strength of GSCE decreases, which could be expected. However, when using a solution with a pH of 4, the strength of GSCE reaches its highest value after 6 cycles, for all  $\text{Na}_2\text{SiO}_3/$

NaOH ratios studied (1.0, 1.5, and 2.0). The results from XRD spectroscopy analysis showed that after 6 cycles in a pH = 4 solution, the sample exhibited the highest crystalline phase of 54.42%, compared to the other w–d cycles, which explained the good performance of GSCE in a pH = 4 solution.

- The FTIR analysis revealed that the sample with  $\text{Na}_2\text{SiO}_3/\text{NaOH} = 1.5$  shows higher transmittance and stronger molecular bonding across various wavenumbers, including the bending vibrations of O–Si–O, constitutional water, OH group, and water stretching. These findings explain why the sample with  $\text{Na}_2\text{SiO}_3/\text{NaOH} = 1.5$  exhibits the maximum compressive strength value compared to those with  $\text{Na}_2\text{SiO}_3/\text{NaOH}$  ratios of 1.0 and 2.0.
- Despite existing studies on the materials used, a comprehensive understanding remains limited. Further research is needed to investigate long-term field exposure under varying conditions, alternative curing methods, and the influence of environmental factors. In addition, aspects such as material cost efficiency, collapse or failure potential, and comprehensive life-cycle assessment have not been sufficiently addressed.

#### References

- [1] Praseeda, K. I., Reddy, B. V. V., Mani, M. "Embodied energy assessment of building materials in India using process and input–output analysis", *Energy and Buildings*, 86, pp. 677–686, 2015.  
<https://doi.org/10.1016/j.enbuild.2014.10.042>
- [2] Asadoullahbar, S. R., Asgari, A., Mohammad Rezapour Tabari, M. "Assessment, identifying, and presenting a plan for the stabilization of loessic soils exposed to scouring in the path of gas pipelines, case study: Maraveh-Tappeh city", *Engineering Geology*, 342, 107747, 2024.  
<https://doi.org/10.1016/j.enggeo.2024.107747>
- [3] Habert, G., d'Espinose de Lacaillerie, J. B., Roussel, N. "An environmental evaluation of geopolymer based concrete production: reviewing current research trends", *Journal of Cleaner Production*, 19(11), pp. 1229–1238, 2011.  
<https://doi.org/10.1016/j.jclepro.2011.03.012>
- [4] Heath, A., Paine, K., McManus, M. "Minimising the global warming potential of clay based geopolymers", *Journal of Cleaner Production*, 78, pp. 75–83, 2014.  
<https://doi.org/10.1016/j.jclepro.2014.04.046>
- [5] Capasso, I., Liguori, B., Ferone, C., Caputo, D., Cioffi, R. "Strategies for the valorization of soil waste by geopolymer production: An overview", *Journal of Cleaner Production*, 288, 125646, 2021.  
<https://doi.org/10.1016/j.jclepro.2020.125646>
- [6] Kasehchi, E., Arjomand, M. A., Alizadeh Elizei, M. H. "Experimental investigation of the feasibility of stabilizing inshore silty sand soil using geopolymer based on ceramic waste powder: An approach to upcycling waste material for sustainable construction", *Case Studies in Construction Materials*, 20, e02979, 2024.  
<https://doi.org/10.1016/j.cscm.2024.e02979>
- [7] Mohseni, E. "Assessment of  $\text{Na}_2\text{SiO}_3$  to NaOH ratio impact on the performance of polypropylene fiber-reinforced geopolymer composites", *Construction and Building Materials*, 186, pp. 904–911, 2018.  
<https://doi.org/10.1016/j.conbuildmat.2018.08.032>
- [8] ASTM "ASTM D6913/D6913M-17 Standard Test Methods for Particle-Size Distribution of Soils Using Sieve Analysis", ASTM International, West Conshohocken, PA, USA, 2017.  
[https://doi.org/10.1520/D6913\\_D6913M-17R25](https://doi.org/10.1520/D6913_D6913M-17R25)
- [9] ASTM "ASTM D854-23 Standard Test Methods for Specific Gravity of Soil Solids by the Water Displacement Method", ASTM International, West Conshohocken, PA, USA, 2023.  
<https://doi.org/10.1520/D0854-23>
- [10] ASTM "ASTM D4318-17e1 Standard Test Methods for Liquid Limit, Plastic Limit, and Plasticity Index of Soils", ASTM International, West Conshohocken, PA, USA, 2017.  
<https://doi.org/10.1520/D4318-17E01>

- [11] ASTM "ASTM D1557-12(2021) Standard Test Methods for Laboratory Compaction Characteristics of Soil Using Modified Effort (56,000 ft-lbf/ft<sup>3</sup> (2,700 kN-m/m<sup>3</sup>))", ASTM International, West Conshohocken, PA, USA, 2021.  
<https://doi.org/10.1520/D1557-12R21>
- [12] AASHTO "AASHTO M 145-91 (2012) Classification of Soil and Soil-Aggregate Mixtures for Highway Construction Purposes", American Association of State Highway and Transportation Officials, Washington, DC, USA, 2012.
- [13] Ngo, T.-P., Phan, V. T.-A., Schwede, D., Nguyen, D.-M., Bui, Q.-B. "Assessing influences of different factors on the compressive strength of geopolymer-stabilised compacted earth", *Journal of the Australian Ceramic Society*, 58(2), pp. 379–395, 2022.  
<https://doi.org/10.1007/s41779-021-00667-1>
- [14] ASTM "ASTM C188-25 Standard Test Method for Density of Hydraulic Cement", ASTM International, West Conshohocken, PA, USA, 2025.  
<https://doi.org/10.1520/C0188-25>
- [15] ASTM "ASTM C618-25a Standard Specification for Coal Ash and Raw or Calcined Natural Pozzolan for Use in Concrete", ASTM International, USA, 2025.  
<https://doi.org/10.1520/C0618-25A>
- [16] Preethi, R. K., Venkatarama Reddy, B. V. "Experimental investigations on geopolymer stabilised compressed earth products", *Construction and Building Materials*, 257, 119563, 2020.  
<https://doi.org/10.1016/j.conbuildmat.2020.119563>
- [17] Yaghoubi, M., Arulrajah, A., Miri Disfani, M., Horpibulsuk, S., Leong, M. "Compressibility and strength development of geopolymer stabilized columns cured under stress", *Soils and Foundations*, 60(5), pp. 1241–1250, 2020.  
<https://doi.org/10.1016/j.sandf.2020.07.005>
- [18] Vo, V.-T., Le, D.-H., Phan, V. T.-A. "Optimisation of alkaline solution for fly ash-sugarcane bagasse ash geopolymer mortars: effects on strength, durability, and microstructure", *European Journal of Environmental and Civil Engineering*, 30(1), 2604297, 2026.  
<https://doi.org/10.1080/19648189.2025.2604297>
- [19] Dheyab, W., Ismael, Z. T., Hussein, M. A., Huat, B. B. K. "Soil Stabilization with Geopolymers for Low Cost and Environmentally Friendly Construction", *GEOMATE Journal*, 17(63), pp. 271–280, 2019.  
<https://doi.org/10.21660/2019.63.8159>
- [20] Hardjito, D., Rangan, B. V. "Development and Properties of Low-calcium Fly Ash Based Geopolymer Concrete", Curtin University of Technology, Perth, Australia, Research Report GC 1, 2005.
- [21] Hardjito, D., Wallah, S. E., Sumajouw, D. M. J., Rangan, B. V. "On the Development of Fly Ash-Based Geopolymer Concrete", *ACI Materials Journal*, 101(6), pp. 467–472, 2004.  
<https://doi.org/10.14359/13485>
- [22] Le, H.-B., Bui, Q.-B., Tang, L. "Geopolymer Recycled Aggregate Concrete: From Experiments to Empirical Models", *Materials*, 14(5), 1180, 2021.  
<https://doi.org/10.3390/ma14051180>
- [23] Ngo, T.-P., Bui, Q.-B., Phan, V. T.-A., Tran, H.-B. "Durability of geopolymer stabilised compacted earth exposed to wetting–drying cycles at different conditions of pH and salt", *Construction and Building Materials*, 329, 127168, 2022.  
<https://doi.org/10.1016/j.conbuildmat.2022.127168>
- [24] Phoo-ngernkham, T., Sinsiri, T. "Workability and Compressive Strength of Geopolymer Mortar from Fly Ash Containing Diatomite", *Engineering and Applied Science Research*, 38(1), pp. 11–26, 2012.
- [25] ASTM "ASTM D2166/D2166M-24 Standard Test Method for Unconfined Compressive Strength of Cohesive Soil", ASTM International, West Conshohocken, PA, USA, 2024.  
[https://doi.org/10.1520/D2166\\_D2166M-24](https://doi.org/10.1520/D2166_D2166M-24)
- [26] ASTM "ASTM D559/D559M-15(2023)e1 Standard Test Methods for Wetting and Drying Compacted Soil-Cement Mixtures", ASTM International, West Conshohocken, PA, USA, 2023.  
[https://doi.org/10.1520/D0559\\_D0559M-15R23E01](https://doi.org/10.1520/D0559_D0559M-15R23E01)
- [27] Singh Rajput, B., Pratap Singh Rajawat, S., Jain, G. "Effect of curing conditions on the compressive strength of fly ash-based geopolymer concrete", *Materials Today: Proceedings*, 103, pp. 32–38, 2024.  
<https://doi.org/10.1016/j.matpr.2023.07.359>
- [28] Khong, T. D., Young, M. D., Loch, A., Thennakoon, J. "Mekong River Delta farm-household willingness to pay for salinity intrusion risk reduction", *Agricultural Water Management*, 200, pp. 80–89, 2018.  
<https://doi.org/10.1016/j.agwat.2017.12.010>
- [29] Van Giang, N., Thanh Dat, N. "Solutions to deal with flooding by using green buildings in Vietnamese urban areas from Japanese experience", *IOP Conference Series: Materials Science and Engineering*, 869(7), 072001, 2020.  
<https://doi.org/10.1088/1757-899X/869/7/072001>
- [30] ASTM "ASTM D4219-22 Standard Test Method for Short-Term Unconfined Compressive Strength Index of Chemically Grouted Soils", ASTM International, West Conshohocken, PA, USA, 2022.  
<https://doi.org/10.1520/D4219-22>
- [31] Abdullah, H. H., Shahin, M. A., Walske, M. L. "Geo-mechanical behavior of clay soils stabilized at ambient temperature with fly-ash geopolymer-incorporated granulated slag", *Soils and Foundations*, 59(6), pp. 1906–1920, 2019.  
<https://doi.org/10.1016/j.sandf.2019.08.005>
- [32] Arulrajah, A., Yaghoubi, M., Disfani, M. M., Horpibulsuk, S., Bo, M. W., Leong, M. "Evaluation of fly ash- and slag-based geopolymers for the improvement of a soft marine clay by deep soil mixing", *Soils and Foundations*, 58(6), pp. 1358–1370, 2018.  
<https://doi.org/10.1016/j.sandf.2018.07.005>
- [33] BSI "BS 5628-1:2005 Code of practice for the use of masonry - Structural use of unreinforced masonry", British Standards Institution, London, UK, 2005.
- [34] Zhou, H., Wang, X., Wu, Y., Zhang, X. "Mechanical properties and micro-mechanisms of marine soft soil stabilized by different calcium content precursors based geopolymers", *Construction and Building Materials*, 305, 124722, 2021.  
<https://doi.org/10.1016/j.conbuildmat.2021.124722>
- [35] Peng, H., Cui, C., Liu, Z., Cai, C. S., Liu, Y. "Synthesis and Reaction Mechanism of an Alkali-Activated Metakaolin-Slag Composite System at Room Temperature", *Journal of Materials in Civil Engineering*, 31(1), 04018345, 2019.  
[https://doi.org/10.1061/\(ASCE\)MT.1943-5533.0002558](https://doi.org/10.1061/(ASCE)MT.1943-5533.0002558)

- [36] Pavithra, P., Srinivasula Reddy, M., Dinakar, P., Hanumantha Rao, B., Satpathy, B. K., Mohanty, A. N. "Effect of the  $\text{Na}_2\text{SiO}_3/\text{NaOH}$  ratio and NaOH Molarity on the Synthesis of Fly Ash-Based Geopolymer Mortar", In: Geo-Chicago 2016: Sustainable Materials and Resource Conservation, Chicago, IL, USA, 2016, pp. 336–344. ISBN 9780784480151  
<https://doi.org/10.1061/9780784480151.034>
- [37] Shihab, A. M., Abbas, J. M., Ibrahim, A. M. "Effects of Temperature in Different Initial Duration Time for Soft Clay Stabilized by Fly Ash Based Geopolymer", Civil Engineering Journal, 4(9), pp. 2082–2096, 2018.  
<https://doi.org/10.28991/cej-03091141>
- [38] Noushini, A., Babae, M., Castel, A. "Suitability of heat-cured low-calcium fly ash-based geopolymer concrete for precast applications", Magazine of Concrete Research, 68(4), pp. 163–177, 2016.  
<https://doi.org/10.1680/macr.15.00065>
- [39] Kamaruddin, F. A., Angraini, V., Kim Huat, B., Nahazanan, H. "Wetting/Drying Behavior of Lime and Alkaline Activation Stabilized Marine Clay Reinforced with Modified Coir Fiber", Materials, 13(12), 2753, 2020.  
<https://doi.org/10.3390/ma13122753>
- [40] Batista dos Santos, G. Z., Passos de Oliveira, D., de Almeida Melo Filho, J., Marques da Silva, N. "Sustainable geopolymer composite reinforced with sisal fiber: Durability to wetting and drying cycles", Journal of Building Engineering, 43, 102568, 2021.  
<https://doi.org/10.1016/j.jobe.2021.102568>
- [41] Oti, J. E., Kinuthia, J. M., Bai, J. "Engineering properties of unfired clay masonry bricks", Engineering Geology, 107(3–4), pp. 130–139, 2009.  
<https://doi.org/10.1016/j.enggeo.2009.05.002>
- [42] Hoy, M., Rachan, R., Horpibulsuk, S., Arulrajah, A., Mirzababaei, M. "Effect of wetting–drying cycles on compressive strength and microstructure of recycled asphalt pavement – Fly ash geopolymer", Construction and Building Materials, 144, pp. 624–634, 2017.  
<https://doi.org/10.1016/j.conbuildmat.2017.03.243>
- [43] Du, Y.-J., Bo, Y.-L., Jin, F., Liu, C.-Y. "Durability of reactive magnesia-activated slag-stabilized low plasticity clay subjected to drying–wetting cycle", European Journal of Environmental and Civil Engineering, 20(2), pp. 215–230, 2016.  
<https://doi.org/10.1080/19648189.2015.1030088>
- [44] Bakharev, T., Sanjayan, J. G., Cheng, Y.-B. "Resistance of alkali-activated slag concrete to acid attack", Cement and Concrete Research, 33(10), pp. 1607–1611, 2003.  
[https://doi.org/10.1016/S0008-8846\(03\)00125-X](https://doi.org/10.1016/S0008-8846(03)00125-X)
- [45] Ayub, F., Khan, S. A. "An overview of geopolymer composites for stabilization of soft soils", Construction and Building Materials, 404, 133195, 2023.  
<https://doi.org/10.1016/j.conbuildmat.2023.133195>
- [46] Venkatarama Reddy, B. V., Prasanna Kumar, P. "Cement stabilised rammed earth. Part B: compressive strength and stress–strain characteristics", Materials and Structures, 44(3), pp. 695–707, 2011.  
<https://doi.org/10.1617/s11527-010-9659-8>